

Preinvasive and invasive ductal pancreatic cancer and its early detection in the mouse

Sunil R. Hingorani,^{1,2} Emanuel F. Petricoin III,³ Anirban Maitra,⁴ Vinodh Rajapakse,⁵ Catrina King,² Michael A. Jacobetz,² Sally Ross,⁵ Thomas P. Conrads,⁶ Timothy D. Veenstra,⁶ Ben A. Hitt,⁷ Yoshiya Kawaguchi,⁸ Don Johann,⁵ Lance A. Liotta,⁵ Howard C. Crawford,⁹ Mary E. Putt,¹⁰ Tyler Jacks,¹¹ Christopher V.E. Wright,⁸ Ralph H. Hruban,⁴ Andrew M. Lowy,¹² and David A. Tuveson^{1,2,*}

¹Department of Medicine

²Department of Cancer Biology
Abramson Family Cancer Research Institute,
Abramson Cancer Center at the University of
Pennsylvania, Philadelphia, Pennsylvania
19103

³FDA-NCI Clinical Proteomics Program,
Center for Biologics Evaluation and Research,
Food and Drug Administration, Bethesda,
Maryland 20892

⁴Departments of Pathology and Oncology,
Sidney Kimmel Cancer Center, Johns Hopkins
University School of Medicine, Baltimore,
Maryland 21287

⁵FDA-NCI Clinical Proteomics Program,
Laboratory of Pathology, National Cancer
Institute, Center for Cancer Research,
Bethesda, Maryland 20892

⁶National Cancer Institute Biomedical
Proteomics Program, Analytical Chemistry
Laboratory, Mass Spectrometry Center, SAIC-
Frederick, Inc., National Cancer Institute at
Frederick, Frederick, Maryland 21702

⁷Correlogic Systems, Inc., Bethesda, Maryland
20892

⁸Department of Cell and Developmental
Biology, Vanderbilt University School of
Medicine, Nashville, Tennessee 37232

⁹Department of Pharmacological Sciences,
State University of New York at Stony Brook,
Stony Brook, New York, 11794

¹⁰Department of Biostatistics and
Epidemiology, University of Pennsylvania,
Philadelphia, Pennsylvania 19104

¹¹Department of Biology, Massachusetts
Institute of Technology, and Howard Hughes

Medical Institute, Center for Cancer Research,
Cambridge, Massachusetts 02139

¹²Department of Surgery, Division of Surgical
Oncology, University of Cincinnati College of
Medicine, Cincinnati, Ohio 45219

*Correspondence: tuvesond@mail.med.upenn.edu

Summary

To evaluate the role of oncogenic *RAS* mutations in pancreatic tumorigenesis, we directed endogenous expression of *KRAS*^{G12D} to progenitor cells of the mouse pancreas. We find that physiological levels of *Kras*^{G12D} induce ductal lesions that recapitulate the full spectrum of human pancreatic intraepithelial neoplasias (PanINs), putative precursors to invasive pancreatic cancer. The PanINs are highly proliferative, show evidence of histological progression, and activate signaling pathways normally quiescent in ductal epithelium, suggesting potential therapeutic and chemopreventive targets for the cognate human condition. At low frequency, these lesions also progress spontaneously to invasive and metastatic adenocarcinomas, establishing PanINs as definitive precursors to the invasive disease. Finally, mice with PanINs have an identifiable serum proteomic signature, suggesting a means of detecting the preinvasive state in patients.

Significance

It is axiomatic in clinical oncology that early detection of cancers increases the likelihood of cure. This is particularly true for pancreatic ductal adenocarcinoma, in which complete resection at even the earliest stage of invasive disease results in dismal long-term prognosis. Understanding the pathogenesis of the preinvasive lesions, termed pancreatic intraepithelial neoplasias (PanINs), and developing the means to detect them therefore represent urgent needs. We have generated a mouse model of PanIN and find that the lesions progress histologically, culminating in fully invasive and metastatic disease. Moreover, we demonstrate a highly reliable means of detecting PanINs in the serum proteome of mutant animals. These results illustrate the potential of genetically engineered mice to accurately model the earliest stages of human neoplasias.

Introduction

Infiltrating ductal adenocarcinoma of the pancreas (PDA) accounts for over 95% of all exocrine pancreatic malignancies and is the fifth-leading cause of cancer-related deaths in the United States. Infiltrating PDA is almost uniformly fatal, with a five-year survival of less than 5% (Warshaw and Fernandez-del Castillo, 1992). The essential incurability of this disease is reflected in virtually identical annual incidence and mortality figures, projected to number 30,300 and 29,700 cases, respectively, for 2003 (Jemal et al., 2003). The median survival for patients with PDA is 4–6 months, in part because the disease usually only becomes clinically apparent at late stages, and because it resists all forms of conventional chemotherapy and radiotherapy. Several factors conspire to obscure the diagnosis of early pancreatic ductal cancer, including the retroperitoneal location of the pancreas and the small size of most of the precursor lesions, which renders them below the detection threshold of current imaging modalities. Even when serendipitously discovered at its earliest stages, and therefore amenable to complete surgical resection, long-term survival is exceedingly rare. The vast majority of even highly selected patients, possessing small primary lesions (less than 2 cm), disease-free resection margins, and negative lymph nodes, inevitably succumb to recurrent or metastatic disease (Allison et al., 1998; Yeo et al., 2002a). Thus, unlike other epithelial malignancies, it appears that from its very inception, PDA is already a micrometastatic disease. Understanding the pathogenesis of the preinvasive state, and developing effective strategies to detect preinvasive pancreatic neoplasms, are therefore of paramount importance.

Similar to long-established models for other epithelial malignancies, such as breast, colon, and prostate, a progression model for the precursor lesions of PDA has been elaborated (Cubilla and Fitzgerald, 1975, 1976; Hruban et al., 2000a; Klimstra and Longnecker, 1994). These lesions, recently codified under the collective term pancreatic intraepithelial neoplasia (PanIN), are grouped into three histologic stages based on increasing degrees of architectural and nuclear atypia (Kern et al.,

2001). A genetic progression model is also emerging which serves to substantiate and illuminate the histological description (Hruban et al., 2000b). Activating mutations in the *KRAS* proto-oncogene are found in over 90% of invasive PDA and are thought to represent an initiating event. Genetic and epigenetic inactivations of a number of tumor suppressor genes, including *p16^{INK4a}*, *p53*, *DPC4* and *BRCA2*, increase in frequency in progressively higher PanIN stages, and culminate in incidences of approximately 90%, 50%–70%, 55%, and 10%, respectively, in invasive PDA. A few heritable predispositions to the disease have been described, involving kindreds with germline mutations in the tumor suppressor genes *p16^{INK4a}*, *BRCA2*, *LKB1*, and *MLH1* (Jaffee et al., 2002). Interestingly, the median age at presentation in these kindreds is not significantly different from sporadic cases, suggesting that these mutations identify genes involved in the progression, and not initiation, of a multigenic process.

A number of tumor suppressor gene knockout and oncogene transgenic mouse models have been developed in recent years incorporating strategies informed by the genetic studies cited above; to date, however, none have recapitulated the features of invasive human PDA or of its noninvasive precursor state. We report here that targeted endogenous expression of a *KRAS^{G12D}* allele to progenitor cells of the mouse pancreas induces ductal lesions that faithfully recapitulate all three stages of human PanINs. These PanINs express proteins that suggest potential targets for chemoprevention and therapy. Moreover, the lesions can spontaneously progress to fully invasive and metastatic ductal adenocarcinoma, with a pattern of spread identical to the human condition, establishing PanINs as definitive precursors to pancreatic ductal cancer. Finally, mice with PanINs have a diagnostic serum proteomic profile that could serve as the basis for detecting the cognate human condition.

Results

Targeting expression of *KRAS^{G12D}* to the mouse pancreas

The ability to target gene expression to different compartments of the mouse pancreas has been aided greatly by recent advances in our understanding of the developmental program of

this vital organ. These studies have identified several transcription factors critical to cellular fate decisions in the developing pancreas (Kim and MacDonald, 2002) (Figure 1A). The first identifiable pancreatic progenitor cells arise in the dorsal and ventral endoderm at embryonic day 8 in the fetal mouse. Expression of *PDX-1/IPF1* occurs around E8.5, and its homozygous deletion is an embryonic lethal event (Offield et al., 1996). *P48/PTF1* is expressed slightly later and is required to commit cells to a pancreatic fate; when it is absent, cells of the developing pancreatic bud instead differentiate into duodenal epithelium (Kawaguchi et al., 2002) and into endocrine cells that migrate to the spleen (Krapp et al., 1998). *P48*^{-/-} animals lack a discernible pancreas and succumb shortly after birth. The *PDX-1* and *P48* double-positive progenitor cells give rise to all the mature cells of the pancreas (Figure 1A). In the adult mouse, *PDX-1* expression is essentially confined to the islet cells, while *P48* is restricted to acinar cells.

To target expression of oncogenic *KRAS* to pancreatic progenitor cells, a conditionally expressed allele was first constructed as previously described (Jackson et al., 2001) (Figure 1B). The targeting vector contains genetic elements that inhibit transcription and translation flanked by functional *LoxP* sites. This *Lox-STOP-Lox (LSL)* construct was inserted into the mouse genomic *KRAS* locus upstream of a modified exon 1 engineered to contain a G → A transition in codon 12. This mutation, commonly found in human PDA, results in a glycine to aspartic acid substitution in the expressed protein, compromising both its intrinsic and extrinsic GTPase activities and resulting in constitutive downstream signaling of Ras effector pathways. Expression of the mutated allele is achieved by interbreeding *LSL-KRAS*^{G12D} mice with animals that express Cre recombinase from the pancreatic-specific promoters, *PDX-1* or *P48*. Lineage tracing studies demonstrate a stochastic pattern of Cre expression in the pancreas of the transgenically derived *PDX-1-Cre* animals, while the knockin strategy used to generate the *P48*^{+Cre} strain results in uniform expression throughout the organ (see Supplemental Figure S1 below). Prior to breeding with Cre-expressing animals, *LSL-KRAS*^{G12D} mice are

functionally heterozygous for the wild-type allele (*KRAS*^{+/-}). Excision of the silencing cassette and subsequent recombination allows for expression of the mutant allele, resulting in a heterozygous mutant condition (*KRAS*^{+G12D}). The excision-recombination event leaves behind a single *LoxP* site, evidence of which can be demonstrated by PCR (Figure 1C). Note that only DNA isolated from the pancreata of these mice, and not from the tails, reveals evidence of recombination.

The pancreata from compound mutant mice are larger than their littermate controls and, particularly in older mice, often have focally nodular parenchyma (Figure 1D). Consistent with expression of the *KRAS*^{G12D} allele, total protein lysates from the pancreata of compound mutant mice contain mutant protein and reveal increased levels of activated, or GTP-bound, Ras (Figure 1E). The slightly higher levels of *Kras*^{G12D} and Ras-GTP in *P48*^{+Cre}; *LSL-KRAS*^{G12D} pancreatic lysates are consistent with expression of the mutant allele throughout the organ. These studies do not, of course, identify the specific cellular compartment(s) within the pancreas that express the *KRAS*^{G12D} allele. Nevertheless, they do establish that the conditional *KRAS*^{G12D} allele is efficiently recombined in the pancreata of *PDX-1-Cre*; *LSL-KRAS*^{G12D} and *P48*^{+Cre}; *LSL-KRAS*^{G12D} compound mutant mice, resulting in expression of the oncogenic protein and elevated Ras-GTP levels.

Endogenous *KRAS*^{G12D} expression induces pancreatic intraepithelial neoplasias (PanINs)

The pancreata of compound mutant mice developed ductal lesions with complete penetrance (33 of 33 animals) that were identical to all three stages of human PanINs. Representative examples of the types of lesions seen in these animals are shown (Figure 2). The normal pancreas is characterized by an abundance of acinar tissue with scattered islets and rarely-seen ducts (Figure 2A). Normal ductal epithelium is comprised of cuboidal cells with uniform round nuclei. Occasionally, so-called reactive ducts, which are thought to reflect injured epithelium, are seen. These ducts are characterized by slightly larger nuclei with less condensed chromatin, but only minimally increased cytoplasm, and are not thought to represent preinvasive lesions (Figure 2B). PanIN-1A lesions are characterized by a transition from

the normal cuboidal morphology to a columnar phenotype with abundant supranuclear, mucin-containing cytoplasm (Figures 2C and 2D). The polarity of these cells is still maintained with basally located nuclei, and nuclear atypia, when seen at all, is minimal. Such lesions were observed in compound mutant mice as young as two weeks old. We note that the development of these lesions was restricted to the small, intralobular ducts of the pancreas, just as in the human condition; the larger interlobular ducts appeared unaffected (Figure 2C). The development of papillary or micropapillary ductal lesions without significant loss of polarity or nuclear atypia identifies them as PanIN-1B (Figures 2E and 2F). Importantly, the pancreata of affected animals retained their overall organotypic architecture with abundant normal-appearing acini and islets.

As the mice aged, higher-grade PanINs were observed with increasing frequency. Moderate nuclear atypia and a loss of polarity, manifested by movement away from a strictly basal location of nuclei, herald the transition to PanIN-2 lesions (Figures 2G and 2H). In PanIN-3 lesions, significant nuclear atypia and complete loss of polarity are observed, such that it is often not possible within the center of one of these lesions to discern luminal from basal boundaries (Figures 2I–2L). Goblet cells, mucus-producing cells normally restricted to respiratory and intestinal epithelia, were seen in PanINs of various stages, but most frequently in PanIN-3 lesions. Though not part of the formal diagnostic criteria for PanINs, they are an associated hallmark of human PanINs and are consistent with the notion of an undifferentiated or inappropriately differentiated pancreatic ductal epithelium toward a more intestinal phenotype. In the PanIN-3 lesions shown here, nuclear enlargement and pleomorphism are apparent; in addition, clusters of cells can be seen which appear to have “budded off” into the lumen. These represent cardinal features of human PanIN-3 lesions, also referred to as carcinoma-in-situ.

In many of the older mice, the pancreata contained extensive ductal lesions, and the acinar parenchyma was largely replaced by an intense stromal, or desmoplastic, reaction

comprised of inflammatory cells, fibroblasts, and collagen deposition (Figures 2I–2K). This fibroinflammatory reaction is highly reminiscent of that seen in human pancreatic cancers and may be secondary to luminal obstruction from the intraductal proliferations. A similar spectrum of ductal lesions was seen with both *PDX-1-Cre;LSL-KRAS^{G12D}* and *P48^{+Cre};LSL-KRAS^{G12D}* mice. We conclude, therefore, that the targeted recombination of a conditional *KRAS^{G12D}* allele in pancreatic progenitor cells induces the full spectrum of pancreatic intraepithelial neoplasias, and substantiates the *KRAS^{G12D}* mutation as an initiating event in pancreatic cancer.

PDX-1-Cre;LSL-KRAS^{G12D} animals did occasionally develop additional tumors with varying penetrance (Supplemental Table S1), including mucocutaneous papillomas (not shown), intestinal metaplasia of the gastric epithelium (Supplemental Figures S2A and S2B), and hyperplastic polyps of the duodenum (Supplemental Figures S2C and S2D). The occurrence of these lesions of the gastrointestinal epithelium likely reflects the expression of *PDX-1* in foregut endothelium progenitor cells during development (Offield et al., 1996). Consistent with this expression pattern, recombination of the conditional allele was detected in the stomach and small bowel, in addition to the pancreas, of *PDX-1-Cre;LSL-KRAS^{G12D}* mice, as well as in cutaneous papillomas but not normal adjacent skin (Supplemental Figure S2E). With one exception, full necropsies of *P48^{+Cre};LSL-KRAS^{G12D}* animals did not reveal extrapancreatic pathology (Supplemental Table S1). One animal displayed evidence of duodenal hyperplasia (not shown), perhaps a result of haploinsufficiency of *P48* in *P48^{+Cre}* mice. In lineage-tracing studies in *P48^{+lacZ}* mice, rare *P48*-expressing cells were retained in the duodenum, the presumed result of insufficient levels of p48 to secure the pancreatic specification of this region of the developing foregut endoderm (Kawaguchi et al., 2002). The relative infrequency of such events is also reflected in the lack of detectable recombination of the *LSL-KRAS^{G12D}* allele in the duodena of most *P48^{+Cre};LSL^{G12D}* animals (Supplemental Figure S2F).

Characterization of PanINs

The proliferative index of PanINs was assessed by expression of PCNA. In wild-type animals, the basal level of PCNA expression was low, measuring $0.55 \pm 0.05\%$ in ducts, $0.94 \pm 0.14\%$ in

acini, and 0% in islets. By comparison, in *PDX-1-Cre;LSL-KRAS^{G12D}* and *P48^{+Cre};LSL-KRAS^{G12D}* animals, 16% ± 1.8% and 22% ± 3.0%, respectively, of ductal cells in PanINs expressed PCNA (Figure 3A). The proliferative index of acinar cells in compound mutant animals was also increased, though to a much lesser degree than PanINs: 3.0 ± 0.6% of acinar cells in *PDX-1-Cre;LSL-KRAS^{G12D}* mice were PCNA-positive, while 6.7 ± 0.8% PCNA-positive acinar cells were observed in *P48^{+Cre};LSL-KRAS^{G12D}* animals. Neither the normal ductal cells nor islet cells in either cohort of compound mutant animals showed any increase in PCNA expression (Figure 3B). Importantly, pancreata from compound mutant animals did not express detectable levels of *p21^{CIP1/WAF1}*, a cell cycle inhibitor and p53 target gene (Figure 3C), arguing against the possibility that the decreased proliferative rates of acinar and islet cells compared with PanINs were due to Ras-induced senescence in the former cell compartments (Serrano et al., 1997).

The epithelial nature of the observed PanINs was confirmed by intense expression of cytokeratin-19 (CK-19), an epithelial cell marker (Figures 3D). Consistent with human PanINs, and with their presumptive status as precursors of adenocarcinomas, an abundant mucin content of PanINs in compound mutant animals was demonstrated by intense Alcian blue staining (Figure 3E) and by immunoreactivity to the mucin-specific protein, Muc5 (Figure 3F). Finally, we note that PanINs expressed only low levels of *PDX-1*, which can nevertheless be discerned when compared to the lack of expression in surrounding acini (Figures 2G and 2H) and to normal ducts in control animals (Figure 2I). Moderate expression of *PDX-1* was observed in duodenal crypts, again consistent with the observation of allelic recombination in the small bowel noted earlier, while high levels of *PDX-1* expression were restricted to the endocrine cells of both control and compound mutant adult animals, as expected (Figures 3G–3I).

PanINs show evidence of histologic progression

To determine more rigorously if the PanINs progress histologically, the total number of ductal lesions and their grade were scored in representative pancreatic sections of cohorts of *PDX-1-Cre;LSL-KRAS^{G12D}* mice of varying age (Figure 4). To decrease the likelihood of scoring the same potentially serpentine duct more than once, only the highest-grade lesion per pancreatic lobule was evaluated. Reactive ducts were not counted as true PanINs. Only lesions that satisfied the accepted criteria for PanIN grades 1–3 were scored as such. It should be noted that a fair degree of variability exists in total tumor burden among mice of the same age, even among littermates. This variability may reflect the inherently unpredictable nature of transgenic expression of the Cre enzyme in *PDX-1-Cre* mice. This caveat notwithstanding, several points were readily apparent. Both the total number of PanINs and their grade clearly increased with advancing age of the mice (Figure 4). In animals 5 months of age or less, the vast majority of ducts were normal. When observed, ductal lesions were largely PanIN-1A. Specifically, at 2.25 months, >80% of ducts were normal; this percentage decreased to 68% at 4–5 months ($p < .089$, using Poisson regression). By 7–10 months, however, more neoplastic (82% of total) than normal ducts were observed ($p < 1 \times 10^{-8}$ compared with 2 months, $p < 1.5 \times 10^{-4}$ compared with 4.5 months). Although the neoplastic ducts still largely consisted of low-grade (1A and 1B) lesions (65%), a substantial number of grade 2 lesions (16%) and the first PanIN-3 lesions could now be seen. Relative to the total number of ducts, the incidence of high-grade (2 and 3) PanINs in the oldest cohort was significantly increased when compared with both young ($p < 7 \times 10^{-5}$) and intermediate-aged mice ($p < 4 \times 10^{-4}$), largely because high-grade lesions were rarely if ever observed in mice younger than 5 months. Similar overall findings were noted in cohorts of *P48^{+Cre};LSL-KRAS^{G12D}* mice.

PanINs activate normally quiescent pathways

We next sought to examine these lesions with specific regard to pathways that offer potential therapeutic and/or chemopreventive targets. The *Notch* signaling pathway is involved in determining cellular fate in the embryonic

development of a variety of tissues (Artavanis-Tsakonas et al., 1999), as well as in the pathological state associated with Alzheimer's disease (Fortini, 2002). Although apparently necessary for the early development of the pancreas, *Notch* signaling is normally suppressed in the adult organ (Apelqvist et al., 1999; Jensen et al., 2000). Very recently, this pathway has been identified as inappropriately upregulated in human pancreatic cancer specimens (Miyamoto et al., 2003). Activation of this pathway can be assessed by nuclear expression of one of its downstream target genes, the transcription factor *Hes1*. PanIN lesions demonstrated strong nuclear expression and faint cytoplasmic expression of *Hes1* (Figure 5A). Nuclear expression was not seen in the normal ducts or islet cells of compound mutant animals, or in these compartments in control animals (Figure 5B); expression in rare centroacinar cells was occasionally seen (not shown) as has been described previously (Miyamoto et al., 2003).

PanINs also expressed increased levels of cyclooxygenase 2, a component of the prostaglandin pathway involved in the inflammatory response. Elevated *COX2* expression has been described in both human PanINs (Maitra et al., 2002) and invasive PDA (Maitra et al., 2002; Tucker et al., 1999). Intense immunohistochemical labeling for Cox-2 was observed in the cytoplasm of PanINs, but not in the ductal cells of control animals (Figures 5C and 5D). Acini and islets revealed varying, but substantially decreased, levels of *COX2* expression.

Finally, we investigated the expression of matrix metalloproteinase-7 (*MMP-7*), a member of the family of zinc-dependent extracellular proteases (Brinckerhoff and Matrisian, 2002). Homozygous deletion of *MMP-7* has been shown to inhibit tumorigenesis (Wilson et al., 1997), while transgenic overexpression can promote it (Rudolph-Owen et al., 1998). Inappropriate *MMP-7* expression has also been identified in preinvasive and invasive human pancreatic cancer specimens (Crawford et al., 2002). We found focally elevated expression of *MMP-7* in a subset of PanIN lesions, but not in the normal ducts or other cells of the pancreas (Figures 5E and 5F), similar to the pattern of

expression seen in human specimens. Interestingly, and again as noted in human pancreata, *MMP-7* expression did not appear to correlate with PanIN grade.

Progression to invasive and metastatic ductal adenocarcinoma

In a cohort of animals ($n = 29$) being followed longitudinally for evidence of disease progression, two mice, one *PDX-1-Cre;LSL-KRAS^{G12D}* (aged 6.25 months) and one *P48^{+Cre};LSL-KRAS^{G12D}* (aged 8.25 months), have thus far developed and succumbed to invasive and metastatic pancreatic ductal adenocarcinoma. Both mice developed locally invasive disease and metastases to the liver. The *PDX-1-Cre;LSL-KRAS^{G12D}* animal developed additional sites of metastatic disease and will be described in greater detail.

At necropsy, a profuse hemorrhagic ascites was noted. The pancreas was large, firm, and fibrotic, and appeared to be encasing the small bowel (Figure 6A). Nodular densities were observed on the liver, diaphragm, and pleural surfaces. Histologic assessment of the pancreas revealed a diffusely infiltrative adenocarcinoma with scattered low and high grade PanINs (Figures 6B–6D). A predominantly glandular pattern of differentiation was noted (Figures 6E and 6F), although there were significant areas of more poorly differentiated carcinoma as well (Figure 6G). The regions manifesting glandular differentiation, in particular, expressed high levels of CK-19, confirming their epithelial nature (Figure 6H). These more well-differentiated regions of the tumor also reacted with Alcian blue and with mucicarmine, a mucin-specific stain, establishing their designation as a glandular mucin-producing carcinoma, or adenocarcinoma (not shown).

The liver contained numerous scattered metastatic lesions which clearly revealed glandular differentiation (Figures 6I and 6J) and which also were CK-19-positive (Figure 6K). A similar histologic appearance and epithelial character was demonstrated by metastases to the lung parenchyma (Figure 6L) and pleural surfaces (Figures 6M and 6N). Several identified peripancreatic lymph nodes had been infiltrated by tumor cells (Figure 6O), and finger-like projections of tumor cells had invaded into the diaphragm (Figure 6P). A metastatic lesion to the adrenal cortex was also noted (not shown).

The presence of neural and vascular invasion in human pancreatic ductal cancer portends an especially poor prognosis, and invasion of nervous plexi is a major source of patient morbidity, resulting in severe and often intractable pain. Invasion of a nervous plexus and encasement of the nerve fibers by tumor cells was observed in this animal as well (Figure 6Q). Cancer cells can be seen completely encasing the nerve fibers and infiltrating the plexus of neuronal cell bodies. Not surprisingly, vascular invasion manifested by infiltration of a vein was also noted (not shown). The sites of metastases observed in this animal are precisely those found in human pancreatic ductal adenocarcinoma and further underscore the accuracy of this mouse model in recapitulating the path to the human disease.

Identification of a proteomic signature in mice with PanIN

Serum proteomic analysis has recently been shown to be an effective means to detect early or recurrent malignancy in patients with ovarian (Petricoin et al., 2002b), breast (Li et al., 2002), and prostate cancer (Adam et al., 2002; Petricoin et al., 2002a). These studies coupled a high-throughput mass spectrometric method, surfaced enhanced laser desorption ionization time-of-flight (SELDI-TOF), with pattern recognition algorithms to detect significant differences that exist between patients and healthy subjects in the low molecular weight range (less than 20,000 MW) of the serum proteome. We wondered whether the serum from PanIN-afflicted animals contained an identifiable proteomic profile that distinguished diseased from normal animals. We note that unfractionated serum was used for these analyses, as it has recently been shown that retention of albumin is essential to the diagnostic power of sera from ovarian and prostate cancer patients, presumably because albumin avidly binds the low MW proteins and concentrates them over time by preventing their otherwise inevitable renal excretion (Liotta et al., 2003).

In a small pilot study designed to establish proof-of-principle, we used a cohort of mice of average age 9.0 ± 0.2 months, which would be expected to have a very high burden of PanINs: based on our previous analyses of

histologic progression (Figure 4), we would expect the vast majority (>80%) of the ducts to contain PanIN lesions. We performed terminal bleeds on a cohort ($n = 12$) of *PDX-1-Cre;LSL-KRAS^{G12D}* and *P48^{+Cre};LSL-KRAS^{G12D}* animals and prepared multiple serum samples from each animal (Table 1). Each animal had extensive, histologically confirmed PanIN, but no evidence of invasive or metastatic disease. Twenty-five age-matched littermate controls (a mix of wild-type, *PDX-1-Cre*, and *P48^{+Cre}* mice) were similarly bled and sacrificed, and were confirmed to have normal pancreata without histologic evidence of PanIN. A total of 25 PanIN serum samples and 40 samples from littermate controls were subjected to SELDI-TOF mass spectrometry to generate an unblinded training set for our bioinformatics algorithm. The resultant model was highly predictive, with a sensitivity of 90.5% (95% CI of 68.3–98.8%) and a specificity of 97.7% (95% CI of 87.7%–99.9%). These results suggested, in principle, that the serum proteome of compound mutant mice with preinvasive pancreatic ductal disease is distinguishable from that of healthy littermate controls.

Having established the potential feasibility of detecting preinvasive pancreatic disease in this small study, we next endeavored to perform a prospective study on a larger set of serially collected samples and subject them to higher resolution mass spectrometry. For these analyses, we used a younger cohort of animals of average age 5.5 ± 0.25 months. The use of younger mice increases the stringency of the test in several ways. First, these animals have a lower total burden of PanINs and a shift toward earlier stage lesions (see Figure 4). Compound mutant mice at this age have a vast majority of normal (67%) as compared with diseased ducts, (33%). Second, and as a direct consequence, such animals are much less likely to have developed invasive ductal cancer. Third, and perhaps most importantly, they have substantially less chronic injury and fibrosis than the older cohort. It is formally possible that the signature identified in the initial pilot study represented the presence of pancreatic fibrosis and not PanIN. Thus, we used this cohort of animals to determine if it was possible to detect very early preinvasive disease and to do so in the relative absence of the underlying fibrosis that accompanies the greater PanIN burden found in older animals.

Independent, serial serum collections were performed on a cohort of 33 compound mutant animals of average age 5.5 ± 0.25 months and 39 aged-matched littermate controls to generate a total of 80 PanIN and 111 control serum samples. All animals were followed for a minimum of three additional weeks after the final serum collection without manifesting overt signs of illness, further decreasing the likelihood that they had developed invasive disease. Training on a subset of 46 PanIN samples and 51 control samples generated a model comprised of 10 specific ion species whose vectorially combined relative intensities were able to accurately distinguish samples from the two populations (Table 2). When tested on a separate blinded set of 34 PanIN samples and 60 controls, the model was able to distinguish cases and controls in this relatively young cohort of mice with a sensitivity of 90% (95% CI of 82.5%–99.9%) and a specificity of 87% (95% CI of 81.6%–99.9%). In addition, we note that samples from *PDX-1-Cre;LSL-KRAS^{G12D}* and *P48^{+Cre};LSL-KRAS^{G12D}* mice were detected with equal fidelity, suggesting that the identified proteomic signature was most likely related to the presence of PanIN and not to the minor extrapancreatic pathology in these animals, which differs between the two cohorts. Thus, these results demonstrate that it is possible to detect even very early preinvasive disease in the serum proteome.

Discussion

The generation of an animal model that incorporates genetic events found in, and faithfully recapitulates the cardinal features of, invasive pancreatic ductal adenocarcinoma, or of the precursor lesions collectively termed pancreatic intraepithelial neoplasias (PanINs), has remained elusive to date. Targeted disruption of a number of tumor suppressor genes believed to be important in human pancreatic oncogenesis, including *p53* (Donehower et al., 1992; Jacks et al., 1994), *p16^{INK4a}* (Serrano et al., 1996), *DPC4* (Sirard et al., 1998), and *BRCA2* (Suzuki et al., 1997), has not yielded any form of pancreatic pathology. The development of oncogenic mutations thought to act as initiating events may therefore represent the rate-limiting step. Two interesting and distinct transgenic mouse

models, each expressing a *KRAS* oncogene from a different heterologous pancreatic-specific promoter, were recently described (Brembeck et al., 2003; Grippo et al., 2003). Although these mice did exhibit varying degrees and types of pancreatic pathology, they too failed to recapitulate the signature features of PDA or of PanIN. We, too, have previously engineered a mouse to overexpress *KRAS^{G12D}* from the acinar-cell specific *MIST-1* promoter. These mice exhibit widespread acinar metaplasia and develop a mixed exocrine pancreatic cancer with cystic, acinar, and ductal features (■■■). Finally, transgenic overexpression of TGF α in acinar cells also results in acinar-to-ductal metaplasia (Sandgren et al., 1990; Wagner et al., 1998). When placed in a *p53*-deficient background, these mice develop an invasive disease that recapitulates some important features of human pancreatic cancer; however, this progression does not occur through histologically defined PanIN lesions, and the relationship of this model to human pancreatic carcinogenesis remains unclear (Wagner et al., 2001). We have demonstrated here that targeted endogenous expression of an oncogenic *KRAS* allele in the mouse pancreas initiates the development of PanINs identical to all three stages found in the cognate human condition. At low frequency, mice with PanIN spontaneously develop both locally invasive adenocarcinoma and metastatic disease, with sites of spread exactly as found in human pancreatic cancer, underscoring both the relevance of this model and establishing PanINs as bona fide precursors to pancreatic ductal adenocarcinoma.

Transgenic animal models differ from those targeting endogenous gene expression in several important ways. First, the random nature of transgene insertion into the host genome results in unpredictable positional effects on levels of expression. Second, in constructs driven by heterologous promoters, the normal physiological regulation of gene expression governed by the endogenous promoter is lost. The cellular effects of oncogenic *RAS* have been shown to be exquisitely dependent upon both the levels and context of *RAS* expression in a number of experimental systems (Shields et al., 2000). In a variety of cell types, ectopic overexpression of *RAS* induces cell cycle arrest and senescence in the absence of cooperating tumor suppressor or oncogenic mutations (Land et al., 1983; Ruley, 1983; Serrano et al., 1997). Conversely, endogenous expression of *KRAS^{G12D}* in mouse embryo fibroblasts (MEFs) stimulates

proliferation and induces focus formation in culture without evidence of additional karyotypic events (D.A.T. et al., submitted). Moreover, targeted expression of this allele in the mouse lung causes hyperproliferative lesions that progress from adenomas to adenocarcinomas (Jackson et al., 2001). These findings are consistent with the presumptive role of activating *RAS* mutations as initiating events in a number of malignancies.

During the preparation of this manuscript, the description of a model involving conditional endogenous expression of another oncogenic *KRAS* allele (*KRAS*^{G12V}) was reported. This model employed a bicistronic allele (*KRAS*^{G12V-IRES- β -geo}) created by targeting a fused IRES- β -geo cassette to the 3' untranslated region of a mutated *KRAS* locus (Guerra et al., 2003). Interestingly, when bred with transgenic *CMV-Cre* animals, expression of activated *KRAS* from this modified allele failed to induce pancreatic lesions or gastric epithelial hyperplasias in mice even up to 8 months of age, despite demonstrated translation of the bicistronic transcript by X-gal staining. Low-grade pancreatic lesions, described by the authors as ductal metaplasia, were seen only in the context of an additional mutation in a cyclin-dependent kinase, *CDK4*^{R24C} (*Cdk4*^{R24C} has a markedly decreased binding affinity for p16^{INK4a} and thereby resists its tumor suppressor affects). On the other hand, the transgenic ectopic expression of *KRAS*^{G12V} from an epithelial-specific CK-19 promoter induces the formation of gastric mucous neck cell hyperplasias, and some pancreatic ductal hyperplasias, but fails to recapitulate the true spectrum of PanINs (Brembeck et al., 2003). Together with the findings reported here, these studies confirm that both the levels of *RAS* expression and the cellular context conspire to determine biological outcome. It may be that the biological consequences of *KRAS*^{G12V} and *KRAS*^{G12D} oncogenes are distinct or, alternatively, that strain-specific effects are responsible for some of the differences discussed here. However, it is also possible that the unusual configuration of the bicistronic allele affects the expression and/or terminal splicing of the *KRAS* transcript, thereby decreasing the overall levels of oncogenic *RAS*, or changing the relative ratio

of the alternatively spliced *KRAS-4A* and *KRAS-4B* transcripts. Indeed, it has been shown that introduction into the mouse genome of a bicistronic construct, directing expression from a single promoter of genes separated by an IRES, results in markedly decreased expression levels of both transcripts compared with separate constructs driven by independent promoters (Jankowsky et al., 2001).

In our system, excision of the silencing cassette upstream of an introduced *KRAS*^{G12D} mutation can occur in pancreatic progenitor cells early in development, and in the islet cells (for *PDX-1-Cre* crosses) or acinar cells (for *P48-Cre* crosses) of the adult mouse. Thus, the model accounts for the possibility that the initiation of tumorigenesis occurs in tissue stem cell compartments while not precluding the study of such events in differentiated cells (Reya et al., 2001). As noted above, an alternate theory of the genesis of ductal adenocarcinoma in the pancreas involves the metaplastic transdifferentiation of acinar to ductal cells. The robust expression of *Hes1* and low, but detectable, levels of *PDX-1* expression in the PanINs described here are consistent with the notion of a relatively undifferentiated or inappropriately differentiated population of cells; of course, such cells could result from progenitor cells gone awry, or from the dedifferentiation of mature ductal or acinar cells. While we cannot formally exclude the possibility that transdifferentiation of acinar to ductal cells occurs in our model system, several points would at least seem to argue against it being the preferred route to PanINs. First, the overall PanIN burden and progression, cellular histology, activated signaling pathways, and serum proteomic signatures found in *PDX-Cre;LSL-KRAS*^{G12D} and *P48^{Cre};LSL-KRAS*^{G12D} compound mutant mice are highly congruous despite different modes of transmission of the *Cre* allele and consequent expression in adult pancreatic cells. Thus, we see essentially normal acinar and islet compartments, respectively, in each of these model systems. In addition, the knockin of *Cre* behind the *P48* promoter means that, in principle, every cell of the adult pancreas in compound mutant mice has potentially rearranged the oncogenic *KRAS* allele to permit expression. Nevertheless, we see the slowly progressive acquisition of ductal lesions similar to that seen in the transgenic, and hence stochastic, *PDX-1-Cre*-associated model. It may be that acinar-to-ductal transdifferentiation is a relatively slow process that

requires weeks to months in vivo after the activation of oncogenic *KRAS* expression. However, at least in explants of developing pancreatic buds transfected in vitro with *Notch*, the observed transdifferentiation of acinar-like cells occurred within 3–4 days (Miyamoto et al., 2003).

We favor an alternate scheme for the development of PanINs seen here. Pancreatic stem cells periodically undergo either cell division to replenish themselves or enter into a differentiation pathway to replace an end-stage cell. We propose that the periodic diversion of a progenitor cell that expresses the rearranged *KRAS*^{G12D} allele toward differentiation along a ductal pathway provides the basis for the evolution of a PanIN. Differentiation along acinar or islet cell pathways does not provide the proper context for *KRAS*^{G12D} to induce true PanINs. Cellular injury, such as that which accompanies ductal obstruction and associated acute and chronic pancreatitis, stimulates increased entry of progenitor cells into the differentiation pathway and increased numbers of PanINs, which in turn cause further obstruction and injury. Such a scenario would explain the increased tumor burden seen in the knockin *P48*^{+Cre};*LSL-KRAS*^{G12D} mice and is consistent with the increased associated risk of developing pancreatic cancer in patients with chronic pancreatitis (Lowenfels et al., 1993). Experiments are currently underway to formally address whether mature or progenitor cell compartments of the pancreas give rise to PanINs by breeding *LSL-KRAS*^{G12D} mice to mice that express Cre recombinase from the *Elastase* or *Cytokeratin-19* promoters, active in mature acinar and ductal cells, respectively.

The findings of activated *Notch* signaling, as manifested by *Hes1* expression, and increased expression of *COX-2* and *MMP-7* in PanINs each provide a basis for therapeutic and/or chemoprevention strategies, which could first be tested in this model system. Agents that interfere with each of these activities are already in approved or investigational use in the clinic. For example, inhibitors of γ -secretase, one of the required proteases in transducing Notch receptor signaling, are currently in clinical trials for Alzheimer's disease (Josien, 2002). The use of nonsteroidal anti-inflammatory drugs has been associated

with a decreased incidence in pancreatic cancer (Anderson et al., 2002), which together with the increased expression of Cox-2 observed here in ductal lesions suggests that Cox-2 activity may represent an important part of the program of events initiated by oncogenic *KRAS*. Finally, matrix metalloproteinases have traditionally been thought to be important for late stages of tumorigenesis involving invasion and metastasis and, accordingly, MMP inhibitors have been used in a number of trials encompassing a variety of metastatic malignancies (Coussens et al., 2002). Unfortunately, these trials were largely unsuccessful. Given the expression of MMP-7 in early-stage PanINs, it may be that these agents would be more efficacious in earlier stages of disease or as chemopreventive agents.

There are currently no tests, radiographic, endoscopic, or serologic, with sufficient sensitivity and specificity to detect pancreatic cancer early enough to effect cures (Hingorani and Tuveson, 2003; Rosty and Goggins, 2002). The most commonly used biomarker of invasive pancreatic cancer, CA 19-9 (carbohydrate antigen), is useful only for following disease progression or response to therapy (Yeo et al., 2002b). Indeed, in a recent prospective study of patients with clinically suspected pancreatic malignancy but no radiographically evident mass, the sensitivity and specificity of CA 19-9 to detect the invasive cancer were only 67% and 88%, respectively (Urgell et al., 2000). The very notion of early detection requires reassessment for pancreatic cancer, however, as even resection of stage I invasive disease affords negligible 10-year survival (Allison et al., 1998). In the absence of therapies that kill metastatic pancreatic cancer cells, which apparently arise from the inception of malignant transformation, the only hope for cures lies in the detection and eradication of the preinvasive state. It is, of course, currently impossible to develop a serologic test for PanIN in patients because of the conundrum of being unable to distinguish those that harbor the lesions from those who do not. We have shown here in an animal model of PanIN that a defining serum proteomic signature exists. Remarkably, this signature was detectable even in mice with very early-stage preinvasive lesions and low overall burden of disease. Further analyses of the key ion species identified in the mass spectrographs may reveal proteins that could form the basis for specific serologic assays. In principle, it may even be possible to use the proteomic

patterns derived from this mouse model to identify similar patterns in patients with PanIN.

Finally, we believe that this model of PanIN represents a suitable platform upon which to build more accurate models of invasive pancreatic adenocarcinoma. The inability to routinely sample pancreatic tissue has challenged the elaboration of histologic and genetic models of progression for human PDA. Thus, it has not been possible to directly chronicle the evolution of ductal pancreatic cancer with serial biopsies, as has been done with colorectal cancer, for example (Fearon and Vogelstein, 1990). A large body of evidence, accumulated over several decades from resected and autopsy specimens, has led to a very useful conceptual model of preinvasive disease involving progression through discrete stages. Though compelling, the model is per force circumstantial. The development, described here, of invasive and metastatic pancreatic ductal adenocarcinoma in older mice harboring PanINs demonstrates unequivocally that these lesions predispose to fully invasive disease. Moreover, the slow progression and low frequency of invasive ductal cancers in these animals would appear to mimic the development of such cancers in humans and presumably reflects the stepwise acquisition of additional mutations in the setting of an expanded pool of proliferating cells. The favorable kinetics of this natural progression should afford the opportunity to dissect the molecular events involved. On the other hand, we would anticipate that establishing endogenous *KRAS*^{G12D} expression in the background of conditionally deleted or mutated alleles of tumor suppressor genes known to be important in human pancreatic oncogenesis would hasten the development of invasive PDA. Indeed, using the *LSL-KRAS*^{G12D} mice described here, it has recently been shown that pancreatic expression of oncogenic *KRAS* cooperates with concomitant *INK4a/ARF* deficiency to induce PDA with very short latency and high penetrance (Aguirre et al., in press). The relative contributions of each of the associated tumor suppressor gene mutations can be systematically evaluated in this fashion.

In summary, we have developed an accurate model of human PanIN in the mouse that faithfully recapitulates the cardinal features of this precursor to invasive pancreatic cancer. The presence of PanINs can be detected accurately in the serum proteome of mutant mice. The fidelity of the model is affirmed by the spontaneous development of fully invasive and metastatic ductal adenocarcinomas. Thus, the model provides a unique platform to study mechanisms of disease pathogenesis, to develop detection and therapeutic strategies for preinvasive disease in high-risk patient populations, and to systematically evaluate multigenic models of invasive and metastatic pancreatic cancer.

Experimental procedures

Mouse strains

The conditional *LSL-KRAS*^{G12D} mice (Jackson et al., 2001) and *P48*^{+/Cre} mice (Kawaguchi et al., 2002) were previously described. *PDX-I-Cre* transgenic mice were generated by injecting fertilized FVB/N oocytes with the *PDX-I-Cre* transgene, and founder mice were identified that expressed Cre in a mosaic pattern in the pancreas, as assessed in the background of a r26 Cre reporter.

KRAS^{G12D} allele recombination and Ras-GTP assays

The recombined *KRAS*^{G12D} allele was identified by PCR as previously described (Jackson et al., 2001). Ras-GTP was precipitated with Raf-GST and detected by immunoblotting per the manufacturer's instructions (UBI). Kras^{G12D} protein was detected by specific antiserum (Johnson et al., 2001).

Histology and immunohistochemistry

Paraffin embedded murine tissues were processed by standard methods. Additional details are provided in the Supplemental Data below.

Statistical analyses

Statistical analyses were carried out using Splus version 6.0 and Stata 8.0. See the Supplemental Data for details.

Serum proteomics

Serum preparation, mass spectroscopy, and pattern recognition data analyses were performed as

previously described (Petricoin et al., 2002b). Further details are supplied in the Supplemental Data.

Acknowledgments

We acknowledge the assistance of Michael Ray in producing the Pdx-1 antibody; Dr. Q.C. Yu and the AFCRI histology core; and Dr. Deborah Silberg, Dr. Gary Swain, and the NIH/NIDDK Center for Molecular studies in Digestive and Liver Diseases (P30 DK050306) and its Morphology Core and Cell Culture facilities. We thank Dr. N. Volkan Adsy (Wayne State University) for performing Muc5 immunohistochemistry and Dr. Tetsuo Sudo for providing the anti-Hes1 antibody. Supported in part by NCI R25-CA87812 (S.R.H.); Johns Hopkins University Clinical Scientist Award (A.M.); NCI P50-CA-62924 (R.H.H.); and McCabe Foundation, Abramson Cancer Center of the University of Pennsylvania Pilot Projects Program, American Cancer Society IRG-78-002-26 and AACR-PanCAN Career Development Award (D.A.T.).

Received: September 12, 2003

Revised: November 26, 2003

Published: December 10, 2003

References

- Adam, B.L., Qu, Y., Davis, J.W., Ward, M.D., Clements, M.A., Cazares, L.H., Semmes, O.J., Schellhammer, P.F., Yasui, Y., Feng, Z., and Wright, G.L., Jr. (2002). Serum protein fingerprinting coupled with a pattern-matching algorithm distinguishes prostate cancer from benign prostate hyperplasia and healthy men. *Cancer Res.* *62*, 3609–3614.
- Allison, D.C., Piantadosi, S., Hruban, R.H., Dooley, W.C., Fishman, E.K., Yeo, C.J., Lillemoe, K.D., Pitt, H.A., Lin, P., and Cameron, J.L. (1998). DNA content and other factors associated with ten-year survival after resection of pancreatic carcinoma. *J. Surg. Oncol.* *67*, 151–159.
- Anderson, K.E., Johnson, T.W., Lazovich, D., and Folsom, A.R. (2002). Association between nonsteroidal anti-inflammatory drug use and the incidence of pancreatic cancer. *J. Natl. Cancer Inst.* *94*, 1168–1171.
- Apelqvist, A., Li, H., Sommer, L., Beatus, P., Anderson, D.J., Honjo, T., Hrabe de Angelis, M., Lendahl, U., and Edlund, H. (1999). Notch signalling controls pancreatic cell differentiation. *Nature* *400*, 877–881.
- Artavanis-Tsakonas, S., Rand, M.D., and Lake, R.J. (1999). Notch signaling: Cell fate control and signal integration in development. *Science* *284*, 770–776.
- Brembeck, F.H., Schreiber, F.S., Deramaudt, T.B., Craig, L., Rhoades, B., Swain, G., Grippo, P., Stoffers, D.A., Silberg, D.G., and Rustgi, A.K. (2003). The mutant K-ras oncogene causes pancreatic periductal lymphocytic infiltration and gastric mucous neck cell hyperplasia in transgenic mice. *Cancer Res.* *63*, 2005–2009.
- Brinckerhoff, C.E., and Matrisian, L.M. (2002). Matrix metalloproteinases: A tail of a frog that became a prince. *Nat. Rev. Mol. Cell Biol.* *3*, 207–214.
- Coussens, L.M., Fingleton, B., and Matrisian, L.M. (2002). Matrix metalloproteinase inhibitors and cancer: trials and tribulations. *Science* *295*, 2387–2392.
- Crawford, H.C., Scoggins, C.R., Washington, M.K., Matrisian, L.M., and Leach, S.D. (2002). Matrix metalloproteinase-7 is expressed by pancreatic cancer precursors and regulates acinar-to-ductal metaplasia in exocrine pancreas. *J. Clin. Invest.* *109*, 1437–1444.
- Cubilla, A.L., and Fitzgerald, P.J. (1975). Morphological patterns of primary nonendocrine human pancreas carcinoma. *Cancer Res.* *35*, 2234–2248.
- Cubilla, A.L., and Fitzgerald, P.J. (1976). Morphological lesions associated with human primary invasive nonendocrine pancreas cancer. *Cancer Res.* *36*, 2690–2698.
- Donehower, L.A., Harvey, M., Slagle, B.L., McArthur, M.J., Montgomery, C.A., Jr., Butel, J.S., and Bradley, A. (1992). Mice deficient for p53 are developmentally normal but susceptible to spontaneous tumours. *Nature* *356*, 215–221.
- Fearon, E.R., and Vogelstein, B. (1990). A genetic model for colorectal tumorigenesis. *Cell* *61*, 759–767.
- Fortini, M.E. (2002). Gamma-secretase-mediated proteolysis in cell-surface-receptor signalling. *Nat. Rev. Mol. Cell Biol.* *3*, 673–684.
- Grippo, P.J., Nowlin, P.S., Demeure, M.J., Longnecker, D.S., and Sandgren, E.P. (2003). Preinvasive pancreatic neoplasia of ductal phenotype induced by acinar cell targeting of mutant Kras in transgenic mice. *Cancer Res.* *63*, 2016–2019.
- Guerra, C., Mijimolle, N., Dhawahir, A., Dubus, P., Barradas, M., Serrano, M., Campuzano, V., and Barbacid, M. (2003). Tumor induction by an endogenous K-ras oncogene is highly dependent on cellular context. *Cancer Cell* *4*, 111–120.
- Hingorani, S.R., and Tuveson, D.A. (2003). In search of an early warning system for pancreatic cancer. *Cancer Biol. Ther.* *2*, 84–86.

- Hruban, R.H., Goggins, M., Parsons, J., and Kern, S.E. (2000a). Progression model for pancreatic cancer. *Clin. Cancer Res.* *6*, 2969–2972.
- Hruban, R.H., Wilentz, R.E., and Kern, S.E. (2000b). Genetic progression in the pancreatic ducts. *Am. J. Pathol.* *156*, 1821–1825.
- Jacks, T., Remington, L., Williams, B.O., Schmitt, E.M., Halachmi, S., Bronson, R.T., and Weinberg, R.A. (1994). Tumor spectrum analysis in p53-mutant mice. *Curr. Biol.* *4*, 1–7.
- Jackson, E.L., Willis, N., Mercer, K., Bronson, R.T., Crowley, D., Montoya, R., Jacks, T., and Tuveson, D.A. (2001). Analysis of lung tumor initiation and progression using conditional expression of oncogenic K-ras. *Genes Dev.* *15*, 3243–3248.
- Jaffee, E.M., Hruban, R.H., Canto, M., and Kern, S.E. (2002). Focus on pancreas cancer. *Cancer Cell* *2*, 25–28.
- Jankowsky, J.L., Slunt, H.H., Ratovitski, T., Jenkins, N.A., Copeland, N.G., and Borchelt, D.R. (2001). Co-expression of multiple transgenes in mouse CNS: A comparison of strategies. *Biomol. Eng.* *17*, 157–165.
- Jemal, A., Murray, T., Samuels, A., Ghafoor, A., Ward, E., and Thun, M.J. (2003). Cancer statistics, 2003. *CA Cancer J. Clin.* *53*, 5–26.
- Jensen, J., Pedersen, E.E., Galante, P., Hald, J., Heller, R.S., Ishibashi, M., Kageyama, R., Guillemot, F., Serup, P., and Madsen, O.D. (2000). Control of endodermal endocrine development by Hes-1. *Nat. Genet.* *24*, 36–44.
- Johnson, L., Mercer, K., Greenbaum, D., Bronson, R.T., Crowley, D., Tuveson, D.A., and Jacks, T. (2001). Somatic activation of the K-ras oncogene causes early onset lung cancer in mice. *Nature* *410*, 1111–1116.
- Josien, H. (2002). Recent advances in the development of gamma-secretase inhibitors. *Curr. Opin. Drug Discov. Dev.* *5*, 513–525.
- Kawaguchi, Y., Cooper, B., Gannon, M., Ray, M., MacDonald, R.J., and Wright, C.V. (2002). The role of the transcriptional regulator Ptf1a in converting intestinal to pancreatic progenitors. *Nat. Genet.* *32*, 128–134.
- Kern, S., Hruban, R., Hollingsworth, M.A., Brand, R., Adrian, T.E., Jaffee, E., and Tempero, M.A. (2001). A white paper: The product of a pancreas cancer think tank. *Cancer Res.* *61*, 4923–4932.
- Kim, S.K., and MacDonald, R.J. (2002). Signaling and transcriptional control of pancreatic organogenesis. *Curr. Opin. Genet. Dev.* *12*, 540–547.
- Klimstra, D.S., and Longnecker, D.S. (1994). K-ras mutations in pancreatic ductal proliferative lesions. *Am. J. Pathol.* *145*, 1547–1550.
- Krapp, A., Knofler, M., Ledermann, B., Burki, K., Berney, C., Zoerkler, N., Hagenbuchle, O., and Wellauer, P.K. (1998). The bHLH protein PTF1-p48 is essential for the formation of the exocrine and the correct spatial organization of the endocrine pancreas. *Genes Dev.* *12*, 3752–3763.
- Land, H., Parada, L.F., and Weinberg, R.A. (1983). Tumorigenic conversion of primary embryo fibroblasts requires at least two cooperating oncogenes. *Nature* *304*, 596–602.
- Li, J., Zhang, Z., Rosenzweig, J., Wang, Y.Y., and Chan, D.W. (2002). Proteomics and bioinformatics approaches for identification of serum biomarkers to detect breast cancer. *Clin. Chem.* *48*, 1296–1304.
- Liotta, L.A., Ferrari, M., and Petricoin, E. (2003). Clinical proteomics: Written in blood. *Nature* *425*, 905.
- Lowenfels, A.B., Maisonneuve, P., Cavallini, G., Ammann, R.W., Lankisch, P.G., Andersen, J.R., Dimagno, E.P., Andren-Sandberg, A., and Domellof, L. (1993). Pancreatitis and the risk of pancreatic cancer. International Pancreatitis Study Group. *N. Engl. J. Med.* *328*, 1433–1437.
- Maitra, A., Ashfaq, R., Gunn, C.R., Rahman, A., Yeo, C.J., Sohn, T.A., Cameron, J.L., Hruban, R.H., and Wilentz, R.E. (2002). Cyclooxygenase 2 expression in pancreatic adenocarcinoma and pancreatic intraepithelial neoplasia: an immunohistochemical analysis with automated cellular imaging. *Am. J. Clin. Pathol.* *118*, 194–201.

- Miyamoto, Y., Maitra, A., Ghosh, B., Zechner, U., Argani, P., Iacobuzio-Donahue, C.A., Sriuranpong, V., Iso, T., Meszoely, I.M., Wolfe, M.S., et al. (2003). Notch mediates TGF alpha-induced changes in epithelial differentiation during pancreatic tumorigenesis. *Cancer Cell* 3, 565–576.
- Offield, M.F., Jetton, T.L., Labosky, P.A., Ray, M., Stein, R.W., Magnuson, M.A., Hogan, B.L., and Wright, C.V. (1996). PDX-1 is required for pancreatic outgrowth and differentiation of the rostral duodenum. *Development* 122, 983–995.
- Petricoin, E.F., 3rd, Ornstein, D.K., Paweletz, C.P., Ardekani, A., Hackett, P.S., Hitt, B.A., Velasco, A., Trucco, C., Wiegand, L., Wood, K., et al. (2002a). Serum proteomic patterns for detection of prostate cancer. *J. Natl. Cancer Inst.* 94, 1576–1578.
- Petricoin, E.F., Ardekani, A.M., Hitt, B.A., Levine, P.J., Fusaro, V.A., Steinberg, S.M., Mills, G.B., Simone, C., Fishman, D.A., Kohn, E.C., and Liotta, L.A. (2002b). Use of proteomic patterns in serum to identify ovarian cancer. *Lancet* 359, 572–577.
- Reya, T., Morrison, S.J., Clarke, M.F., and Weissman, I.L. (2001). Stem cells, cancer, and cancer stem cells. *Nature* 414, 105–111.
- Rosty, C., and Goggins, M. (2002). Early detection of pancreatic carcinoma. *Hematol. Oncol. Clin. North Am.* 16, 37–52.
- Rudolph-Owen, L.A., Chan, R., Muller, W.J., and Matrisian, L.M. (1998). The matrix metalloproteinase matrilysin influences early-stage mammary tumorigenesis. *Cancer Res.* 58, 5500–5506.
- Ruley, H.E. (1983). Adenovirus early region 1A enables viral and cellular transforming genes to transform primary cells in culture. *Nature* 304, 602–606.
- Sandgren, E.P., Luetkeke, N.C., Palmiter, R.D., Brinster, R.L., and Lee, D.C. (1990). Overexpression of TGF alpha in transgenic mice: induction of epithelial hyperplasia, pancreatic metaplasia, and carcinoma of the breast. *Cell* 61, 1121–1135.
- Serrano, M., Lee, H., Chin, L., Cordon-Cardo, C., Beach, D., and DePinho, R.A. (1996). Role of the INK4a locus in tumor suppression and cell mortality. *Cell* 85, 27–37.
- Serrano, M., Lin, A.W., McCurrach, M.E., Beach, D., and Lowe, S.W. (1997). Oncogenic ras provokes premature cell senescence associated with accumulation of p53 and p16INK4a. *Cell* 88, 593–602.
- Shields, J.M., Pruitt, K., McFall, A., Shaub, A., and Der, C.J. (2000). Understanding Ras: 'it ain't over 'til it's over'. *Trends Cell Biol.* 10, 147–154.
- Sirard, C., de la Pompa, J.L., Elia, A., Itie, A., Mirtsos, C., Cheung, A., Hahn, S., Wakeham, A., Schwartz, L., Kern, S.E., et al. (1998). The tumor suppressor gene Smad4/Dpc4 is required for gastrulation and later for anterior development of the mouse embryo. *Genes Dev.* 12, 107–119.
- Suzuki, A., de la Pompa, J.L., Hakem, R., Elia, A., Yoshida, R., Mo, R., Nishina, H., Chuang, T., Wakeham, A., Itie, A., et al. (1997). Brca2 is required for embryonic cellular proliferation in the mouse. *Genes Dev.* 11, 1242–1252.
- Tucker, O.N., Dannenberg, A.J., Yang, E.K., Zhang, F., Teng, L., Daly, J.M., Soslow, R.A., Masferrer, J.L., Woerner, B.M., Koki, A.T., and Fahey, T.J., 3rd. (1999). Cyclooxygenase-2 expression is up-regulated in human pancreatic cancer. *Cancer Res.* 59, 987–990.
- Urgell, E., Puig, P., Boadas, J., Capella, G., Queralto, J.M., Boluda, R., Antonijuan, A., Farre, A., Lluís, F., Gonzalez-Sastre, F., and Mora, J. (2000). Prospective evaluation of the contribution of K-ras mutational analysis and CA 19.9 measurement to cytological diagnosis in patients with clinical suspicion of pancreatic cancer. *Eur. J. Cancer* 36, 2069–2075.
- Wagner, M., Luhrs, H., Kloppel, G., Adler, G., and Schmid, R.M. (1998). Malignant transformation of duct-like cells originating from acini in transforming growth factor transgenic mice. *Gastroenterology* 115, 1254–1262.

Wagner, M., Greten, F.R., Weber, C.K., Koschnick, S., Mattfeldt, T., Deppert, W., Kern, H., Adler, G., and Schmid, R.M. (2001). A murine tumor progression model for pancreatic cancer recapitulating the genetic alterations of the human disease. *Genes Dev.* *15*, 286–293.

Warshaw, A.L., and Fernandez-del Castillo, C. (1992). Pancreatic carcinoma. *N. Engl. J. Med.* *326*, 455–465.

Wilson, C.L., Heppner, K.J., Labosky, P.A., Hogan, B.L., and Matrisian, L.M. (1997). Intestinal tumorigenesis is suppressed in mice lacking the metalloproteinase matrilysin. *Proc. Natl. Acad. Sci. USA* *94*, 1402–1407.

Yeo, C.J., Cameron, J.L., Lillemoe, K.D., Sohn, T.A., Campbell, K.A., Sauter, P.K., Coleman, J., Abrams, R.A., and Hruban, R.H. (2002a). Pancreaticoduodenectomy with or without distal gastrectomy and extended retroperitoneal lymphadenectomy for periampullary adenocarcinoma, part 2: Randomized controlled trial evaluating survival, morbidity, and mortality. *Ann. Surg.* *236*, 355–366.

Yeo, T.P., Hruban, R.H., Leach, S.D., Wilentz, R.E., Sohn, T.A., Kern, S.E., Iacobuzio-Donahue, C.A., Maitra, A., Goggins, M., Canto, M.I., et al. (2002b). Pancreatic cancer. *Curr. Probl. Cancer* *26*, 176–275.

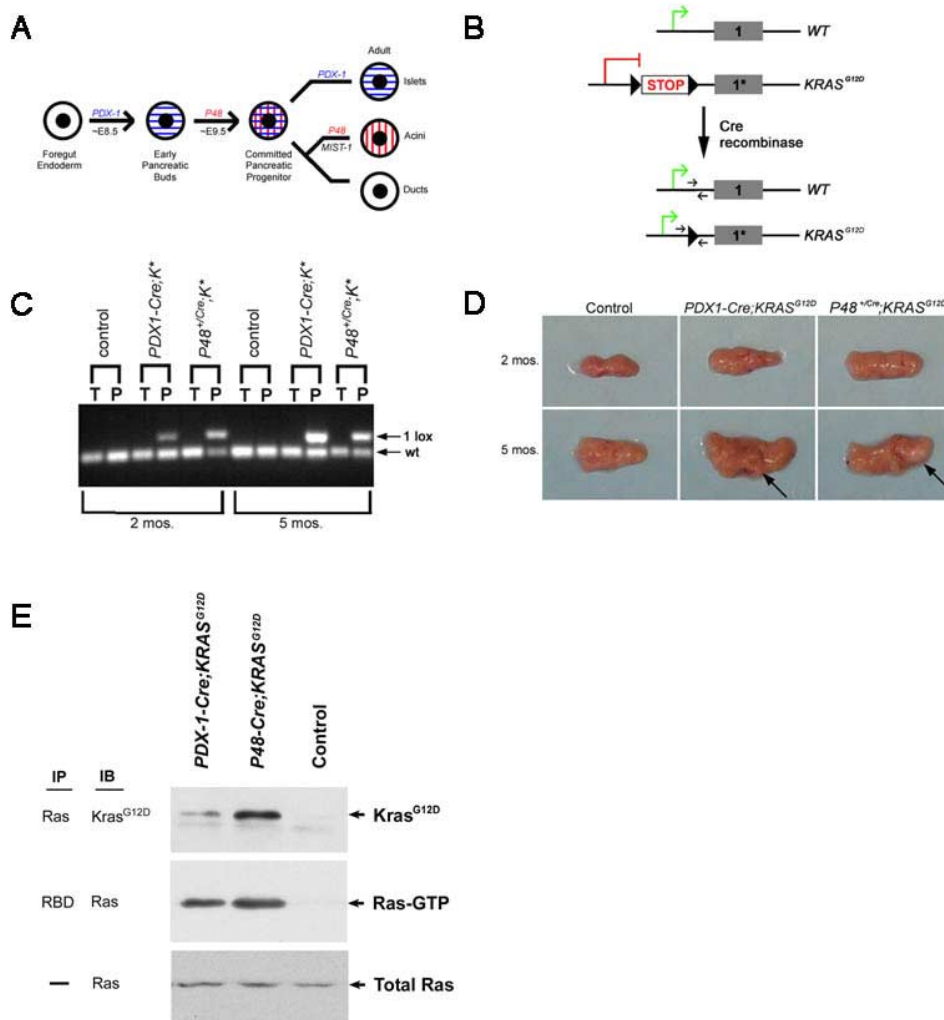


Figure 1. Targeting endogenous *KRAS^{G12D}* expression to the mouse pancreas

A: Simplified schematic diagram of the program of transcription factor expression in the developing mouse pancreas. *PDX-1* expression (blue) is apparent by embryonic day 8.5 (E8.5), while *P48* expression (red) begins on approximately E9.5. The resultant *PDX-1* and *P48* double-positive cells give rise to all of the cells of the mature organ.

B: Conditional *LSL-KRAS^{G12D}* allele and generation of expressed *KRAS^{G12D}* allele after *Cre*-mediated excision-recombination. Arrows indicate relative position of PCR primers used to detect alleles. PCR distinguishes presence of recombined allele from *WT* allele by addition of 40 bp (34 bp for LoxP site plus 6 bp added *Sall* restriction site). A separate reaction is used to detect the presence of the unrecombined conditional allele (not shown).

C: PCR of tail (T) and pancreatic (P) DNA from 2- and 5-month-old *P48^{+Cre};LSL-KRAS^{G12D}*, *PDX-1-Cre;LSL-KRAS^{G12D}*, and littermate control mice. The recombined allele is present in the pancreata but not the tails of compound mutant mice.

D: Pancreata from young (2 months, top panels) and older (5 months, bottom panels) *PDX-1-Cre;LSL-KRAS^{G12D}* and *P48^{+Cre};LSL-KRAS^{G12D}* animals are larger than those of the respective control animals. Arrows indicate pancreatic nodules.

E: Kras^{G12D}, Ras-GTP, and total Ras levels in whole pancreatic lysates of 2-month-old *PDX-1-Cre;LSL-KRAS^{G12D}*, *P48^{+Cre};LSL-KRAS^{G12D}*, and control animals. Detectable levels of Kras^{G12D} and Ras-GTP are seen in compound mutant animals but not in controls.

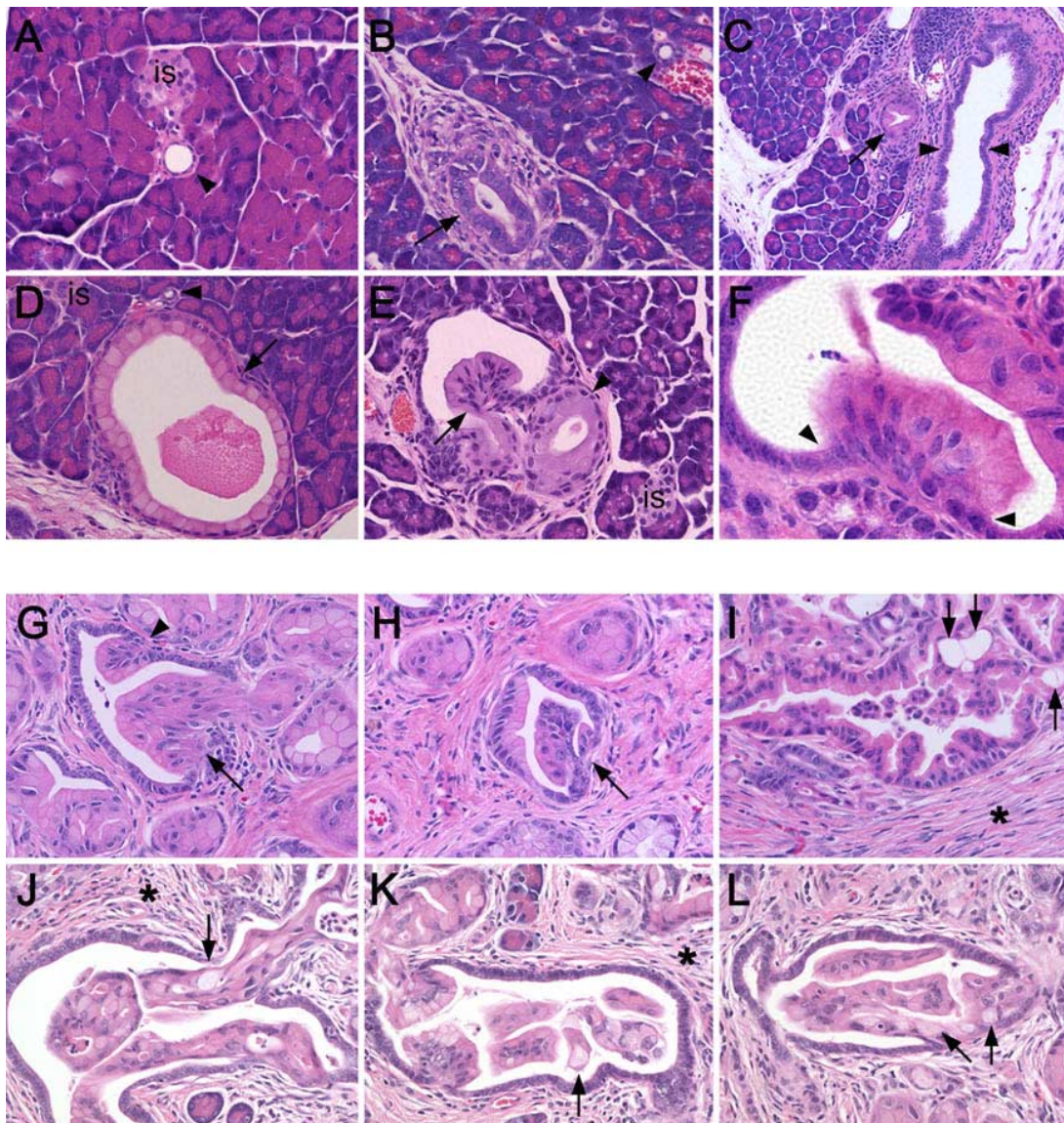


Figure 2. Endogenous *KRAS^{G12D}* expression induces both early- (top panels) and advanced- (bottom panels) stage pancreatic intraepithelial neoplasias (PanINs)

A. Wild-type pancreas revealing normal cuboidal ductal epithelium in cross-section (arrowhead), islet (is), and surrounding acinar tissue (400 \times).

B. Reactive duct (arrow) showing enlarged nuclei and normal duct (arrowhead) in adjacent lobule (400 \times).

C. PanIN-1A in small intralobular duct (arrow) and adjacent normal interlobular duct (delimited by arrowheads). Note the relative sizes of the two ductal structures (200 \times).

D. PanIN-1A (arrow) and adjacent normal duct (arrowhead) and islet (is) (400 \times).

E. PanIN-1B (arrow) showing papillary architecture and an adjacent PanIN-1a (arrowhead) (400 \times).

F. Papillary architecture of PanIN-1B lesion at abrupt transition from more normal appearing ductal epithelium (arrowheads) (1000×).

G and H. Higher-grade PanIN-2 lesions (arrows) reveal more significant loss of polarity and moderate nuclear atypia. In (**G**), an adjacent lesion within the same duct has features more consistent with PanIN-1B (arrowhead, 400×).

I–L. High-grade PanIN-3 lesions reveal complete loss of cellular polarity, significant nuclear atypia, and budding of cell clusters into the ductal lumen. Goblet cells (arrows) are also seen with increasing frequency, as is the surrounding fibroinflammatory reaction (asterisk) (1000×).

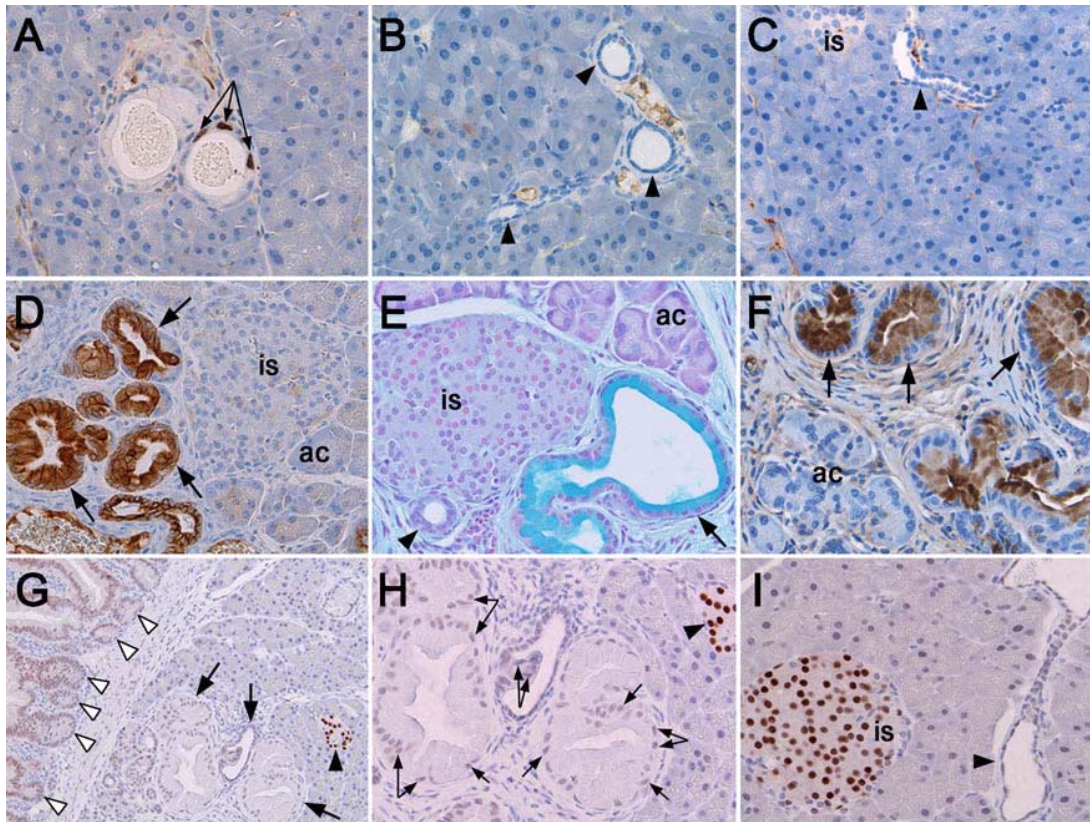


Figure 3. Characterization of PanINs

A: High levels of PCNA expression (arrows) seen in numerous PanINs of a *PDX-1-Cre;LSL-KRAS^{G12D}* mouse but not in surrounding acinar tissue (400 \times).

B: Absence of PCNA expression in normal pancreatic ducts (arrowheads) from the same compound mutant animal as in (A) (400 \times).

C: Absence of p21 immunoreactivity in a normal duct (arrowhead), acini, and islet of a *PDX-1-Cre;LSL-KRAS^{G12D}* mouse (400 \times).

D: Intense expression of epithelial cell marker, cytokeratin-19 (CK-19), in numerous PanINs (examples indicated by arrows) of a compound mutant animal (400 \times).

E: Alcian blue stain reveals abundant mucin content of a PanIN-1A (arrow) which is absent from islets (is), acini (ac), and an adjacent reactive duct (arrowhead) (400 \times).

F: Immunoreactivity to mucin-specific protein, Muc5, is seen in PanINs (arrows), but not in adjacent acini (ac) (400 \times).

G–I: Immunohistochemical detection of *PDX-1* expression in pancreata from *PDX-1-Cre;LSL-KRAS^{G12D}* (**G** and **H**) and control mice (**I**). **G:** Intense nuclear *PDX-1* expression is seen in islets (arrowhead), high-level expression in intestinal crypts (open arrowheads), and faint expression in Pan-INs (arrows, 200 \times). **H:** Higher-power view of **G** (400 \times). **I:** High-level expression in islets (is) but not in ducts (arrowhead) (400 \times).

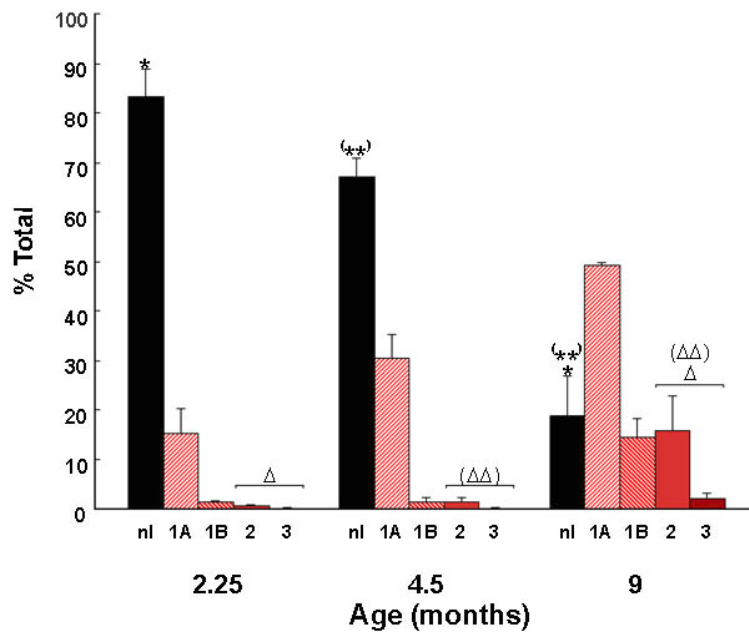


Figure 4. Histologic progression of PanINs in *PDX-1-Cre;LSL-KRAS^{G12D}* mice
 Percentages (\pm SEM) of normal (nl) and neoplastic ducts by grade (1A, 1B, 2, 3) in mice of average age 2.25 months (n = 6), 4.5 months (n = 4), and 9 months (n = 4). p values: *, $< 1 \times 10^{-8}$; **, $< 1.5 \times 10^{-4}$; Δ , 7×10^{-5} ; $\Delta\Delta$, 4×10^{-4} .

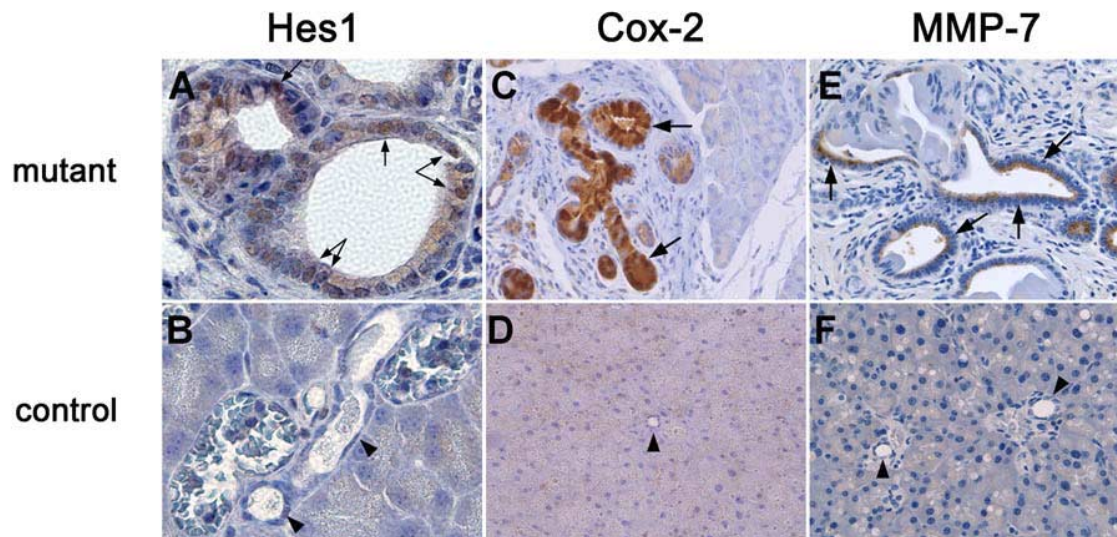


Figure 5. Signaling pathways in PanINs

A and B: Nuclear expression of *Hes1* (arrows) is seen in PanINs (**A**, arrows) but not in normal ducts (**B**, arrowheads) (1000 \times).

C and D: Cytoplasmic expression of *COX-2* is high in PanINs (**C**, arrows), markedly lower in surrounding acini, and absent in control ducts (**D**, arrowhead) (400 \times).

E and F: Focal expression of *MMP-7* is found in PanINs (**E**, arrows). No *MMP-7* expression was observed in the ductal epithelium (**F**, arrowheads) or other structures of control animals (400 \times).

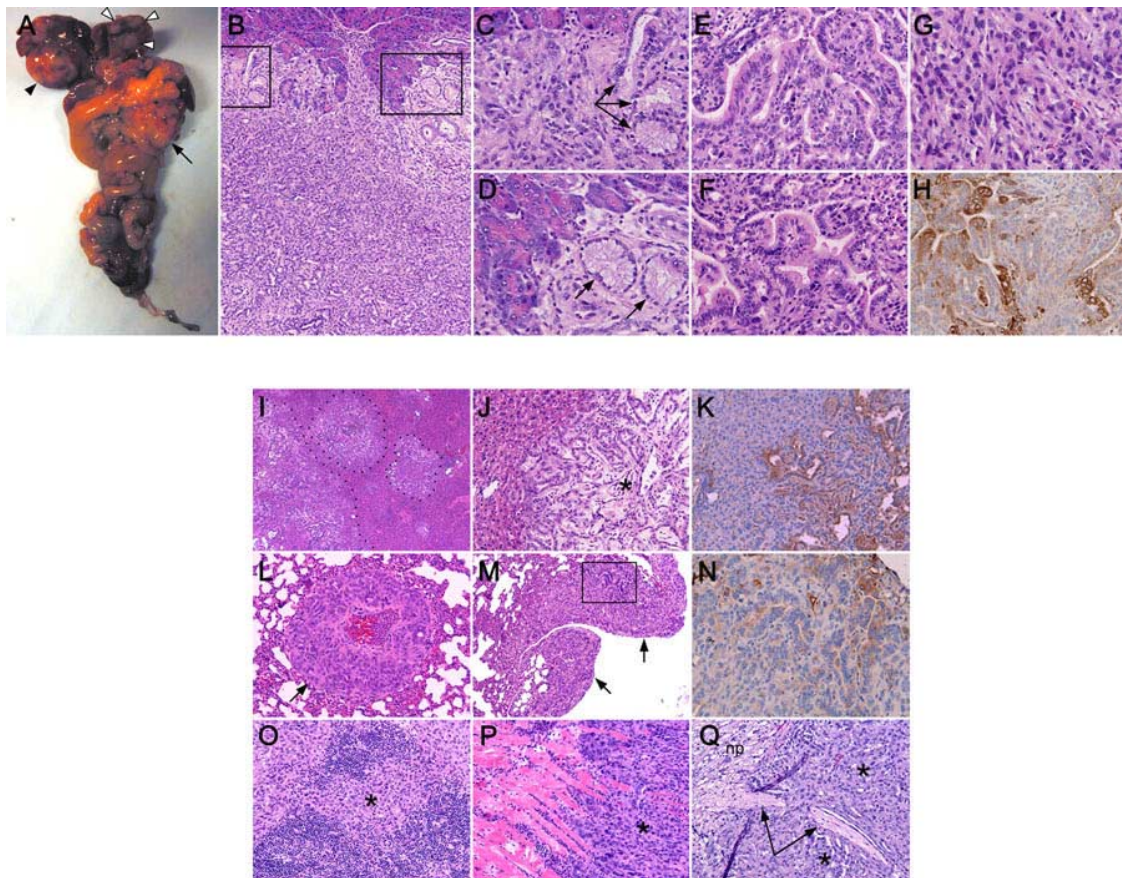


Figure 6. Invasive (top panels) and metastatic (bottom panels) pancreatic ductal adenocarcinoma (PDA) in a *PDX-1-Cre; LSL-KRAS^{G12D}* mouse

A. Gross photograph of abdominal organs. Note the multiple smaller (open arrowheads) and single large (closed arrowhead) liver metastases. The pancreas (arrow) was dramatically enlarged and nodular and encased the small bowel.

B. PDA invading the pancreas, with PanINs (boxes) scattered throughout (40 \times).

C and D. Higher magnifications of PanINs at the border of invasive cancer (400 \times).

E and F. Well-differentiated regions of invasive PDA revealing prominent glandular architecture (400 \times).

G. Region of poorly differentiated PDA within same tumor (400 \times).

H. CK19 expression in well-differentiated region of PDA (400 \times).

I–K. Several distinct liver metastases were noted (**I** [dashed lines, 40 \times] and **J** [asterisk, 200 \times]), and demonstrated immunoreactivity to CK-19 (**K**) (200 \times).

L. Lung metastasis (arrow, 200 \times).

M and N. Pleural nodules (**M**) (arrows, 100 \times) are immunoreactive for the epithelial marker, CK19 (**N**) (400 \times of boxed region).

O. Peripancreatic lymph node metastasis (asterisk, 200 \times).

P. Diaphragmatic invasion by tumor cells in finger-like projections (asterisk, 200 \times).

Q. Neural plexus (np) and associated nerve fibers (arrows) invaded by PDA. The nerve fibers are encased by tumor cells (asterisks, 400×).

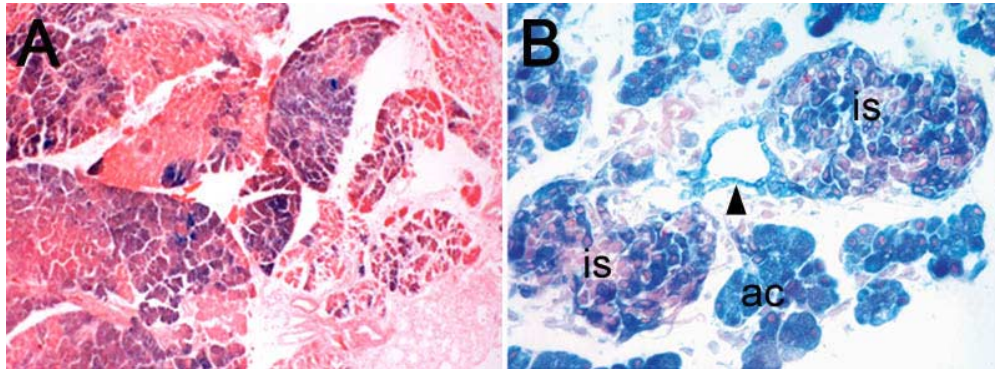
Table 1. Serum proteomic analysis of murine PanIN: Pilot study

Cohort	Age (months)	# mice	# serum samples	Failed QA/QC	Train	Test	Sensitivity	Specificity
PanIN	9.4 ± 0.3	12	48	2	25	21	90.5% (95% CI of 68.3–98.8%)	97.7% (95% CI of 87.7–99.9%)
Control	9.0 ± 0.2	25	100	17	40	43	90.5% (95% CI of 68.3–98.8%)	97.7% (95% CI of 87.7–99.9%)

Table 2. Serum proteomic analysis of murine PanIN: Prospective study

A: Parameters of sample populations								
Cohort	Average age (months)	# mice	# serum samples	Failed QA/QC	Train	Test	Sensitivity	Specificity
PanIN	5.5 ± 0.25	33	95	15	46	34	90% (95% CI of 82.5–99.9%)	87% (95% CI of 81.6–99.9%)
Control	6.5 ± 0.2	39	125	14	51	60	90% (95% CI of 82.5–99.9%)	87% (95% CI of 81.6–99.9%)
B: Parameters of model								
Key ions	<i>m/z</i>							
1	802.8846							
2	2886.9487							
3	4653.8955							
4	7409.861							
5	7849.1104							
6	8284.527							
7	8371.117							
8	9415.561							
9	11495.136							
10	11499.733							

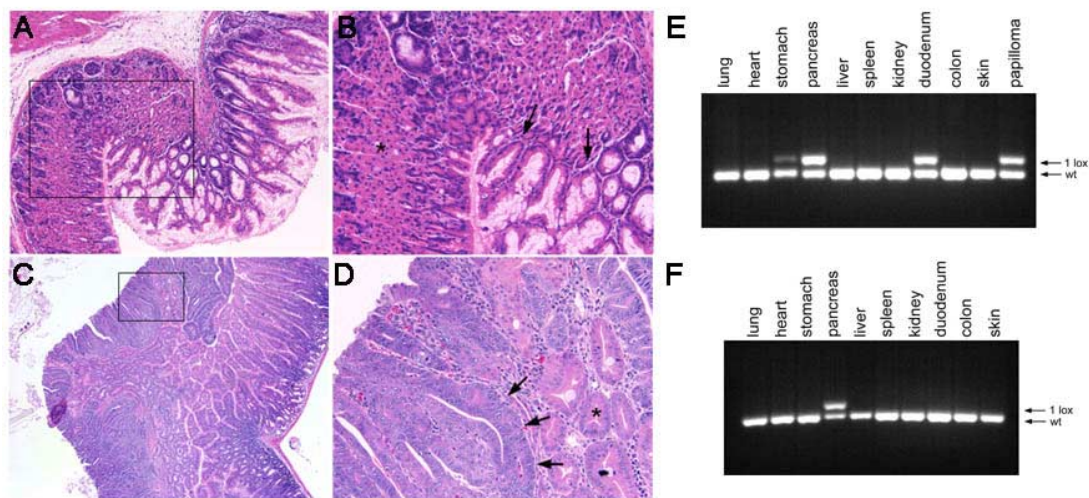
Supplemental data



Supplemental Figure S1. Expression patterns of Cre recombinase in *PDX-1-Cre* and *P48^{+Cre}* animals revealed in combination with r26-LSL-LacZ Cre reporters by XGAL staining

A: Mosaic expression of *PDX-1-Cre* in pancreas (40×).

B: Homogenous pancreatic expression of *P48^{+Cre}* knockin allele (400×).



Supplemental Figure S2. Histological sequelae and molecular evidence of extrapancreatic expression of *KRAS^{G12D}*

A and B: Intestinal metaplasia (**A**, 100×; **B**, 400×) in *PDX-1-Cre; LSL-KRAS^{G12D}* mice. Note the normal stomach (asterisk) and abnormal, mucin filled crypts (arrows).

C and D: Duodenal hyperplasias (**C**, 40×; **D**, 400×) in *PDX-1-Cre; LSL-KRAS^{G12D}* mice. Note the hyperchromatic nuclei (arrows) and abnormal crypts (asterisk).

E: Molecular evidence of recombination in genomic DNA from stomach, pancreas, duodenum, and mucocutaneous papillomas of *PDX-1-Cre; LSL-KRAS^{G12D}* mouse.

F: Molecular evidence of recombination in genomic DNA from pancreas, but not other organs, of *P48^{+Cre}; LSL-KRAS^{G12D}* mouse.

Supplemental experimental procedures

Histology and immunohistochemistry

Unstained 5 μm sections were deparaffinized and placed in Target Retrieval Solution (pH 6.0, Envision Plus Detection Kit, Dako) for 20 min at 100°C. After cooling for 20 min, slides were quenched with 3% hydrogen peroxide for 5 min, followed by primary antibody incubations using the Dako Autostainer. Labeling was detected with the Dako Envision system following the manufacturer's protocol. Negative controls (primary antibody replaced by serum from appropriate species) were used for each antibody in each run. For Pdx-1 immunodetection, antigen retrieval was performed by microwave in citrate buffer at 90°C–95°C and primary antibody incubations were performed O/N at 4°C; labeling was detected with the Vectastain Elite kit (Vecta Labs). Antibodies used: Cox2 (Santa Cruz), PCNA (BD Biosciences), Muc5 (Novacastra), Hes1 (gift of Dr. Tetsuo Sudo), MMP-7 (Crawford et al., 2002), CK19 (PhenoPath), Pdx-1 (guinea pig polyclonal antibody prepared against a GST-Pdx-1 fusion protein and confirmed not to react with pancreatic buds isolated from *PDX-1* deficient mice).

Statistical analyses

Statistical analyses were carried out using Splus version 6.0 and Stata 8.0. Histological progression was evaluated using sample means and standard errors of the mean (SEM). To test for the effect of age, Poisson regression models were constructed that contained the total number of ducts with and without age as independent variables. Analysis of deviance was used to test for an overall effect of age. If the overall effect of age was significant, individual groups (2 versus 4.5-, 2 versus >7-, and 4.5 versus >7-month-old mice) were then compared using Wald tests. All tests were two-sided with a Type I error rate of 0.05. Exact 95% confidence intervals were constructed for the sensitivity and specificity results from the SELDI-TOF data.

Serum proteomics

Whole blood was collected from cohorts of *PDX-1-Cre;LSL-KRAS^{G12D}* and *P48^{+Cre};LSL-KRAS^{G12D}* mice and their littermate controls by accessing the retroorbital plexus. Blood was allowed to clot at room temperature for 45 min and serum collected by benchtop ultracentrifugation (6500 rpm \times 10 min) and stored at –80 C. In an initial pilot study, blood was collected as a terminal event and serum prepared and aliquotted. In a subsequent prospective study, serial blood samples were collected and serum prepared as independent events from a cohort of 33 compound mutant and 39 littermate control animals. Between 1–6 bleeds were performed per animal at intervals of not less than 5 days. A total of 50–100 μl of whole blood was collected per bleed and serum prepared and frozen. Samples were then randomly divided into training and testing sets for subsequent analyses. Testing sets were blinded to the investigators performing the pattern recognition analyses.

Serum mass spectroscopy and pattern recognition data analysis were performed as previously described (Petricoin et al., 2002b). Briefly, thawed unfractionated serum samples were applied to a WCX2 (weak cation exchange protein chip) (CIPHERGEN Biosystems, Fremont, CA), and subjected to SELDI-TOF mass spectrometry on a Protein Biology System 2c (CIPHERGEN Biosystems, Fremont, CA) for the initial pilot study described, or on a QSTAR Pulsar *i* (Applied Biosystems Inc., Framingham, MA) for the prospective study. Data were collected without filters or reduced using peak picking software. The resultant spectral data streams, comprised of peak amplitudes at approximately 15,200 (PBS2c) or 350,000 (QSTAR) mass-to-charge (m/z) ratio positions were exported as .csv files and analyzed by an artificial-intelligence type pattern recognition algorithm (Proteome Quest β version 1.0, Correlogic Systems Inc., Bethesda, MD) after performing quality control (QC) and quality assurance (QA) measures of the spectra. The data streams for the high-resolution spectra (QSTAR) were first binned using a function of 400 parts per million (ppm). The binning process condenses the number of data points from 350,000 to exactly 7,084 points per sample. To perform spectral QC and QA, raw and binned data were subjected to plotting by total ion current (total record count), average/mean and standard deviation of amplitude, chi-square and t test analysis of each ion or bin, and quartile plotting measures using JMP software (SAS Institute, Cary, NC), as well as stored procedures developed in-house. Process measures were checked by analyzing the statistical plots of the

serum reference standard (SRM-015A, National Institutes of Standards and Technology) that applied at random points on each chip at different spot locations. Spectra that failed statistical checks for homogeneity were eliminated from in-depth modeling and analysis.

Pattern recognition analyses on the resultant spectra were performed in two phases: (1) training with known serum samples, and (2) testing validation with blinded samples that had not been used in the training set. In phase I, the genetic algorithm attempts to identify, through a neo-Darwinistic “survival of the fittest” approach, a limited number of clusters in N-dimensional space. The clusters are plots of the Euclidean distance vector, comprised of the combined normalized intensities of the randomly sampled m/z values of the cases and controls, respectively (for more detailed description of the pattern recognition process, please refer to <http://clinicalproteomics.steem.com>). In phase II, masked test spectra are then analyzed and the distance vector calculated and plotted for each sample using only the m/z species comprising the diagnostic model identified in training. N-dimensional plotting yields classification as disease, control, or neither, depending on whether the sample falls into previously existing case or control clusters formed in training, or establishes a new cluster.

Supplemental Table 1: Neoplastic spectrum of *LSL-KRAS^{G12D}* mice in the *PDX-1-Cre* and *P48^{+/-Cre}* backgrounds

Cohort	Mouse	Age (months)	PanIN	Intestinal metaplasia	Duodenal hyperplasias	Papillomas
<i>PDX-1-Cre;KRAS^{G12D}</i>	4804	2	+	+	-	-
	4808	2	+	+	-	-
	3256	3	+	+	-	+
	3143	4	+	+	-	+
	4645	5	+	+	-	+
	4181	5.5	+	+	-	+
	3711	7	+	+	-	+
	3929	8.5	+	+	-	+
	3931	9.5	+	+	+	+
	3145	11	+	+	+	+
<i>P48^{+/-Cre};KRAS^{G12D}</i>	3158	3	+	-	-	-
	4651	4	+	-	-	-
	3710	8	+	-	-	-
	3385	9	+	-	-	-
	3252	9.5	+	-	-	-
	3248	9.5	+	-	-	-
	3160	10	+	-	+	-
	3152	10.5	+	-	-	-
	3156	10.5	+	-	-	-
	3082	11	+	-	-	-